Peer reviewed version

Link to published version (if available):
10.1021/acs.macromol.7b02025

Link to publication record in Explore Bristol Research
PDF-document

University of Bristol - Explore Bristol Research
General rights

Supporting Information

Cylindrical Micelles with "Patchy" Coronas from the Crystallization-Driven Self-Assembly of ABC Triblock Terpolymers with a Crystallizable Central Polyferrocenyldimethylsilane Segment

Alex M. Oliver[†], Jessica Gwyther[†], Mitchell A. Winnik[‡], and Ian Manners[†*]

[†] School of Chemistry, University of Bristol, Bristol, BS8 1TS, UK

[‡] Department of Chemistry, University of Toronto, 80 George Street, Toronto, Ontario M5S 3H6, Canada

* To whom correspondence should be addressed, e-mail: ian.manners@bristol.ac.uk

TECHNIQUES

Unless otherwise stated, all reactions were carried out on an all-glass vacuum line under nitrogen or in an MBraun glovebox under an inert purified nitrogen atmosphere.

^{1}H and ^{13}C NMR spectra were obtained using a Varian 400 MHz spectrometer and all resonances were referenced to residual NMR solvent peaks.

Gel permeation chromatography (GPC) was conducted on a Viscotek VE2001 GPCmax chromatograph equipped with a triple detector array, equipped with automatic sampler, pump, injector, inline degasser, column oven (30 °C), elution columns consisting of styrene/divinylbenzene gels (with pore sizes between 500 Å and 100,000 Å), refractometer (VE 3580), four-capillary differential viscometer, UV/Vis detector (VE 3210, λ = 440 nm) and dual angle laser light scattering detector (VE 270, 7° and 90°). THF (Fisher) was used as the eluent, with the flow rate set at 1 mL/min. Samples were dissolved in the eluent (2 mg/mL) and filtered through a Ministart SRP 15 filter (polytetrafluorethylene membrane, pore size = 0.45 µm) before analysis. The detectors were calibrated using polystyrene standards (Viscotek).

Matrix-assisted laser desorption/ionization time-of-flight (MALDI-TOF) mass spectrometry was performed on a Bruker UltrafleXtreme 4700 instrument. Samples of poly(methyl)methacrylate (PMMA) were prepared by combining a solution of *trans*-2-[3-(4-*tert*-butylphenyl)-2-methyl-2-propenylidene]malononitrile matrix (20 mg/mL in THF), AgOTf (10 mg/mL in THF) with the polymer (2 mg/mL in THF) in a 10:0.5:1 (v/v/v) ratio. All other samples were prepared without the addition of AgOTf using the same concentrations and ratios. Approximately 1.5 µL of the mixed sample was deposited onto a stainless steel plate and allowed to dry in air.

Bright field transmission electron microscopy (TEM) micrographs were obtained on a JEOL JEM 1400 microscope operating at 120 kV and equipped with a Gatan Orius SC1000 CCD camera. Samples were analyzed by drop-casting one drop (*ca*. 8 µL) of the micelle colloidal solution onto a carbon coated copper grid placed upon a piece of filter paper to remove excess solvent. Copper grids (400 mesh) were purchased from Agar Scientific and carbon films were prepared by using a Quorum TEM Turbo Carbon Coater by sputtering carbon onto mica sheets. The carbon films were deposited onto the copper grids by floatation on water and the carbon coated grids were allowed to dry for at least two days in air. Most samples did not require staining; samples that did were stained by exposing a freshly drop-cast sample to an aqueous RuO_4 solution (2 wt%) overnight.

Polydisperse micelle samples were sonicated using a Bandelin Sonorex Digitec DT 255 H sonic bath (ultrasonic nominal output = 160 W).

EXPERIMENTAL PROCEDURES

Solubility Studies of PS and PMMA Homopolymers in Self-Assembly Solvents

5 mg of PS_{143} homopolymer (the aliquot prepared for **1**, M_n = 14.9 kDa, PDI = 1.08) were added to 3

separate 1 mL vials, and 1 mL of DMAA, EtOAc and acetone were added to each of these. This was also

repeated for $PMMA_{188}$ homopolymer (the polymer used for the synthesis of **1**, M_n = 18.8 kDa, PDI =

1.17). The mixtures were stirred for 5 min to study how well the polymers dissolved in the solvents used

for self-assembly.

For PS_{143}, the polymer was soluble in both DMAA and EtOAc, and initially swelled in acetone; after

aging further for 30 min, the polymer was fully dissolved. For PMMA, the polymer was insoluble and did

not swell in DMAA, and soluble in both EtOAc and acetone. Leaving PMMA to age in DMAA over a

further 24 h did not dissolve the polymer. The results were as expected based on the solubility parameters

of the relevant polymers and solvents (see Table S2)

Living CDSA of PS-b-PFS-b-PMMA Triblock Terpolymers

PS homopolymer was added to micelle solutions for some living CDSA experiments with triBCP **2** in an

attempt to alleviate micellar aggregation. This was conducted by diluting a sample of micelles (1 : 1, v/v)

with a solution of PS homopolymer in *n*-butyl acetate (2 mg/mL). Although this was effective, the

contrast between the micelle cores and the PS homopolymer film itself proved problematic to effectively

see a useful number of micelles.

*Block Comicelle Formation with PS-b-PFS-b-PMMA Triblock Terpolymers from PFS-b-P2VP Seed
Micelles*

A THF solution of PS-*b*-PFS-*b*-PMMA triblock terpolymer unimer (5 µL, 10 mg/mL) was added to a

solution of PFS-*b*-P2VP seed micelles (20 µL, 0.1 mg/mL, L_n = 114 nm) diluted in acetone/EtOAc

solvent systems (200 µL). The mixture was stirred gently for 2 s, allowed to age for 24 h and the samples were characterized by TEM.

Block Comicelle Formation with PS-b-PFS-b-PMMA Triblock Terpolymers from Alternative PS-b-PFS-b-PMMA seed micelles

A THF solution of PS-*b*-PFS-*b*-PMMA triblock terpolymer unimer (**1**, 10 µL, 5 mg/mL) was added to a solution of PS-*b*-PFS-*b*-PMMA seed micelles (**2**, 100 µL, 0.5 mg/mL, L_n = 101 nm) diluted in acetone (400 µL). The mixture was stirred gently for 2 s, allowed to age for 24 h and the samples were characterized by TEM. The inverse triblock comicelle sample using seed micelles of **1** (L_n = 92 nm) and a THF solution of **2** (5 mg/mL) was also prepared by the same method.
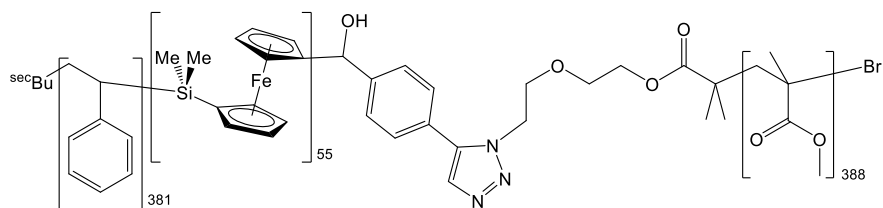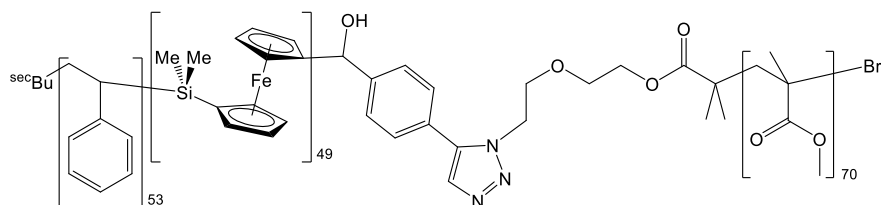
EXPERIMENTAL DATA

PS$_{143}$-*b*-PFS$_{40}$-*b*-PMMA$_{188}$, **1**
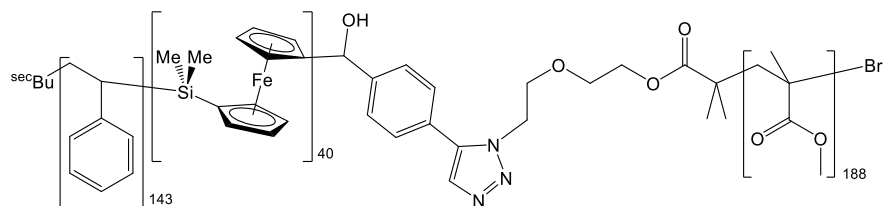
^{1}H NMR (400 MHz, CD$_2$Cl$_2$): 0.56 (s, 6H, Si*Me$_2$*), 0.73-1.28 (br, 3H, α-CC*H$_3$*), 1.34-2.48 (br, 1H, C*H$_2$*C*H*(Ph); 2H, α-CC*H$_2$*), 3.59 (s, 3H, -OC*H$_3$*), 4.12 (m, 4H, *Cp*), 4.28 (m, 4H, *Cp*), 6.41-7.21 (br, 5H, CH$_2$CH(*Ph*)); M_n (GPC) = 60.5 kg/mol, M_w/M_n = 1.13; block ratio = 3.6:1.0:4.7; yield = 38%.

PS$_{381}$-*b*-PFS$_{55}$-*b*-PMMA$_{388}$, **2**

^{1}H NMR (400 MHz, CD$_2$Cl$_2$): 0.56 (s, 6H, Si*Me$_2$*), 0.73-1.28 (br, 3H, α-CC*H$_3$*), 1.34-2.48 (br, 1H, C*H$_2$*C*H*(Ph); 2H, α-CC*H$_2$*), 3.59 (s, 3H, -OC*H$_3$*), 4.12 (m, 4H, *Cp*), 4.28 (m, 4H, *Cp*), 6.41-7.21 (br, 5H, CH$_2$CH(*Ph*)); M_n (GPC) = 88.1 kg/mol, M_w/M_n = 1.13; block ratio = 7.0:1.0:6.9; yield = 43%.

PS$_{53}$-*b*-PFS$_{49}$-*b*-PMMA$_{70}$, **3**

^{1}H NMR (400 MHz, CD$_2$Cl$_2$): 0.56 (s, 6H, Si*Me$_2$*), 0.73-1.28 (br, 3H, α-CC*H$_3$*), 1.34-2.48 (br, 1H, C*H$_2$*C*H*(Ph); 2H, α-CC*H$_2$*), 3.59 (s, 3H, -OC*H$_3$*), 4.12 (m, 4H, *Cp*), 4.28 (m, 4H, *Cp*), 6.41-7.21 (br, 5H, CH$_2$CH(*Ph*)); M_n (GPC) = 24.2 kg/mol, M_w/M_n = 1.05; block ratio = 1.1:1.0:1.4; yield = 33%.
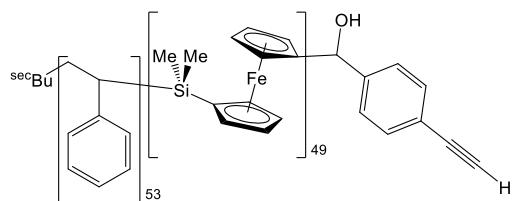

PS$_{143}$-*b*-PFS$_{40}$, **4a**
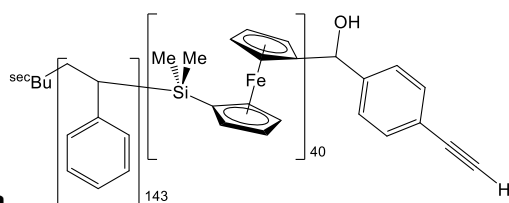
^{1}H NMR (400 MHz, CD$_2$Cl$_2$): 0.56 (s, 6H, Si*Me$_2$*), 1.44-2.48 (br, 1H, C*H$_2$*C*H*(Ph)), 4.12 (m, 4H, *Cp*), 4.28 (m, 4H, *Cp*), 6.41-7.21 (br, 5H, CH$_2$CH(*Ph*)); M_n (GPC) = 24.7 kg/mol, M_w/M_n = 1.04; block ratio = 3.6:1.0; yield = 90%.
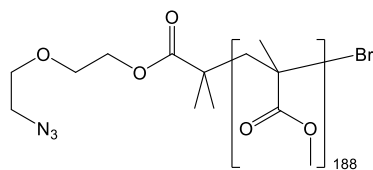
PS$_{381}$-*b*-PFS$_{55}$, **4b**
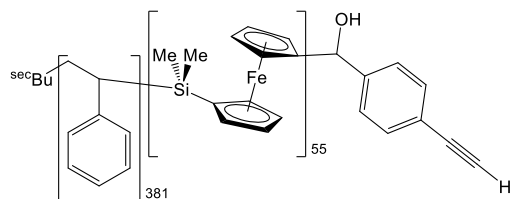
^{1}H NMR (400 MHz, CD$_2$Cl$_2$): 0.56 (s, 6H, Si*Me$_2$*), 1.44-2.48 (br, 1H, C*H$_2$*C*H*(Ph)), 4.12 (m, 4H, *Cp*), 4.28 (m, 4H, *Cp*), 6.41-7.21 (br, 5H, CH$_2$CH(*Ph*)); M_n (GPC) = 53.3 kg/mol, M_w/M_n = 1.06; block ratio = 7.0:1.0; yield = 93%.
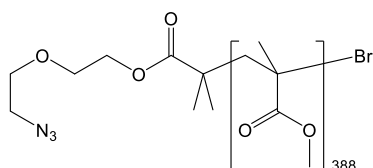
PS$_{53}$-*b*-PFS$_{49}$, **4c**

^{1}H NMR (400 MHz, CD$_2$Cl$_2$): 0.56 (s, 6H, Si*Me$_2$*), 1.44-2.48 (br, 1H, C*H$_2$*C*H*(Ph)), 4.12 (m, 4H, *Cp*), 4.28 (m, 4H, *Cp*), 6.41-7.21 (br, 5H, CH$_2$CH(*Ph*)); M_n (GPC) = 17.5 kg/mol, M_w/M_n = 1.02; block ratio = 1.1:1.0; yield =94%.

PMMA$_{188}$, **5a**

^{1}H NMR (400 MHz, CDCl$_3$): 0.73-1.28 (br, 3H, α-CC*H$_3$*), 1.34-2.10 (br, 2H, α-CC*H$_2$*), 3.59 (s, 3H, -OC*H$_3$*); M_n (GPC) = 18.8 kg/mol, M_w/M_n = 1.17; yield = 58%.

PMMA$_{388}$, **5b**

^{1}H NMR (400 MHz, CDCl$_3$): 0.73-1.28 (br, 3H, α-CC*H$_3$*), 1.34-2.10 (br, 2H, α-CC*H$_2$*), 3.59 (s, 3H, -OC*H$_3$*); M_n (GPC) = 38.1 kg/mol, M_w/M_n = 1.10; yield = 47%.

PMMA$_{70}$, **5c**

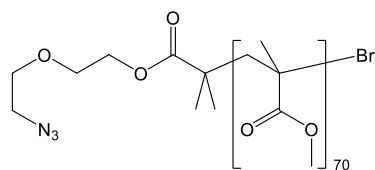^{1}H NMR (400 MHz, CDCl$_3$): 0.73-1.28 (br, 3H, α-CCH_3), 1.34-2.10 (br, 2H, α-CCH_2), 3.59 (s, 3H, -OCH_3); M_n (GPC) = 7.0 kg/mol, M_w/M_n = 1.02; yield = 31%.

SUPPLEMENTARY TABLES AND FIGURES

Table S1. Characterization data of homopolymers and diblock copolymers prepared in the synthesis of PS-*b*-PFS-*b*-PMMA materials, including number-average molecular weight (M_n), degree of polymerisation (DP_n), block ratio and polydispersities (PDI).

Composition	Material	Block Ratio [a]	M_n / kg mol^{-1}	PDI [b]
PS$_{143}$-*b*-PFS$_{40}$ [d]	**4a**	3.6 : 1.0	24.7 [b]	1.04
PS$_{384}$-*b*-PFS$_{55}$ [d]	**4b**	7.0 : 1.0	53.3 [b]	1.06
PS$_{55}$-*b*-PFS$_{49}$ [d]	**4c**	1.1 : 1.0	17.5 [b]	1.02
PMMA$_{188}$ [e]	**5a**	-	18.8 [b,c]	1.17
PMMA$_{381}$ [e]	**5b**	-	38.1 [b,c]	1.10
PMMA$_{70}$ [e]	**5c**	-	7.0 [b,c]	1.02
PS$_{143}$	**6a**	-	14.9 [b,c]	1.08
PS$_{384}$	**6b**	-	40.0 [b,c]	1.09
PS$_{55}$	**6c**	-	5.7 [b,c]	1.03

[a] Determined by ^{1}H NMR through comparative integration of aromatic protons (5H) of PS and methyl protons (6H) of PFS, [b] Determined by GPC with a triple-detector array, [c] Determined by MALDI-TOF [d] alkyne capped, [e] azide capped

Table S2. Hildebrand solubility parameters of homopolymers (left) and solvents (right).[2-4]

Polymer	δ (Mpa)$^{1/2}$	Solvent	δ (Mpa)$^{1/2}$
Polystyrene (PS)	18.5	DMAA[a]	16.8
Poly(ferrocenyldimethylsilane) (PFS)	18.7	Butyl acetate	17.6
Polymethylmethacrylate (PMMA)	19.0	EtOAc[b]	18.1
		THF	18.5
		Acetone	19.9

[a] dimethylacetamide, [b] ethyl acetate

Table S3. Contour length data for cylindrical micelles prepared by seeded growth of unimers of **1** in acetone from seed micelles of **1** ($L_n = 92$ nm, $L_w/L_n = 1.12$).

	Unimer-to-seed ratio						
	0.5	**1**	**2**	**4**	**8**	**14**	**20**
L_n / nm	134	242	317	537	758	1284	2063
L_w / nm	152	265	332	565	780	1298	2090
L_w/L_n	1.13	1.09	1.05	1.05	1.03	1.01	1.01
σ / nm	48	74	68	123	129	137	239

Table S4. Contour length data for cylindrical micelles prepared by seeded growth of unimers of **2** in acetone from seed micelles of **2** (L_n = 101 nm, L_w/L_n = 1.14).

	Unimer-to-seed ratio				
	0.5	**1**	**2**	**4**	**10**
L_n / **nm**	133	191	266	486	1072
L_w / **nm**	139	199	274	507	1115
L_w/L_n	1.05	1.04	1.03	1.04	1.03
σ / nm	29	37	45	100	215

Table S5. Contour length data for cylindrical micelles prepared by seeded growth of unimers of **3** in acetone from seed micelles of **3** (L_n = 88 nm, L_w/L_n = 1.09).

	Unimer-to-seed ratio				
	1	**2**	**4**	**6**	**8**
L_n / **nm**	218	329	598	733	854
L_w / **nm**	229	344	610	755	878
L_w/L_n	1.05	1.05	1.02	1.03	1.03
σ / nm	49	70	110	129	138
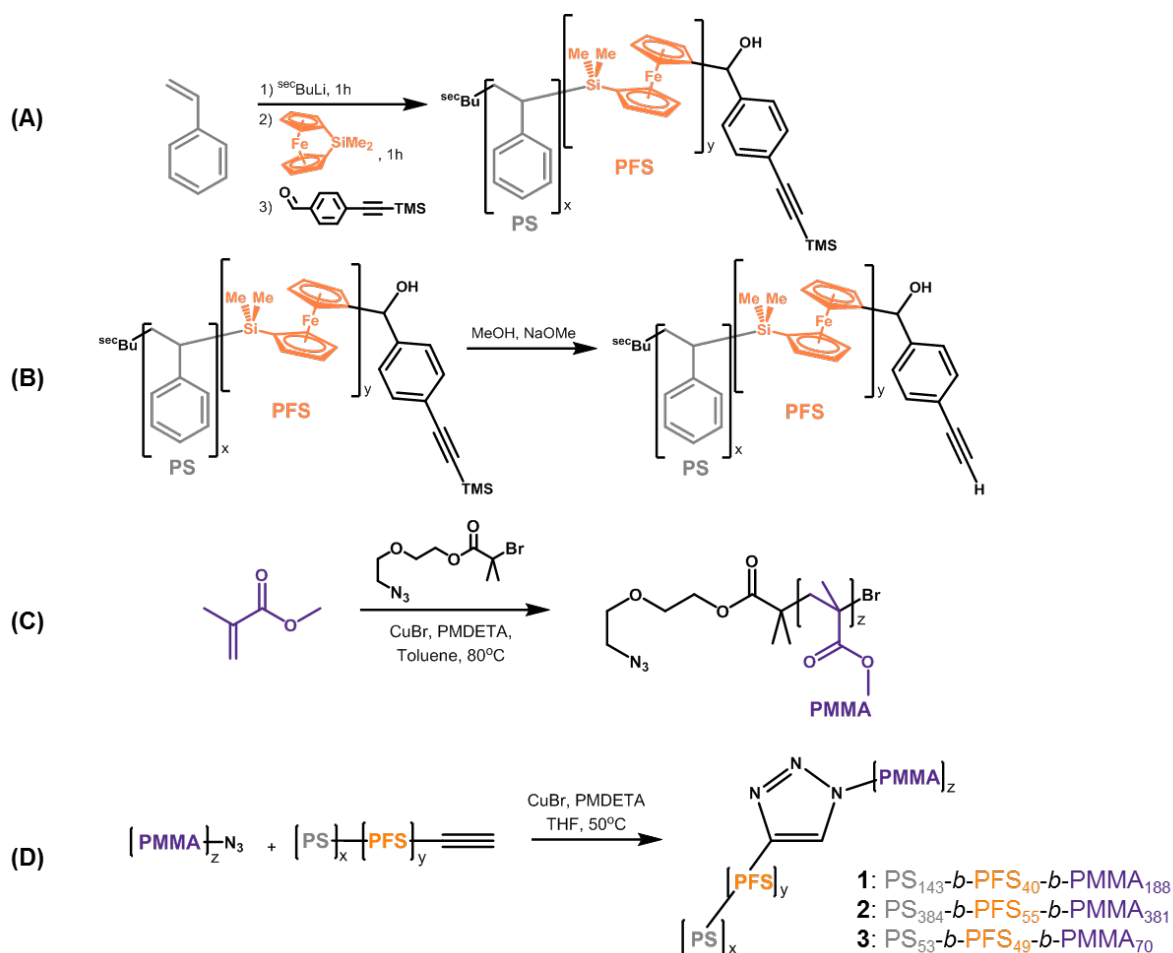
Scheme S1. Generalised synthesis for the formation of PS-*b*-PFS-*b*-PMMA triblock terpolymers; (A) reaction procedure for the sequential living anionic polymerisation[1] and (B) subsequent deprotection of the protected alkyne end-group for the preparation of PS-*b*-PFS-alkyne BCPs; (C) reaction procedure for the atom-transfer radical polymerisation (ATRP) methyl methacrylate with an azide-functionalized initiator for the preparation of PMMA-azide; (D) reaction procedure for the azide/alkyne Huisgen (CuAAC) cycloaddition "Click" of PS-*b*-PFS-alkyne and PMMA-azide for the synthesis of PS-*b*-PFS-*b*-PMMA triblock terpolymers.[5] DP$_n$ for each polymer is outlined in Table S1.
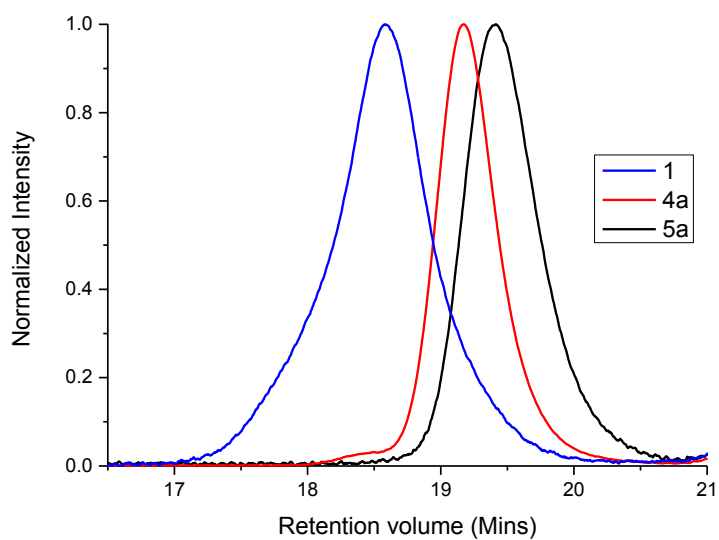
Figure S1. GPC chromatographs (refractive index response) in THF of purified triblock terpolymer **1** (PS$_{143}$-*b*-PFS$_{40}$-*b*-PMMA$_{188}$), and its precursors **4a** (PS$_{143}$-*b*-PFS$_{40}$) and **5a** (PMMA$_{188}$).
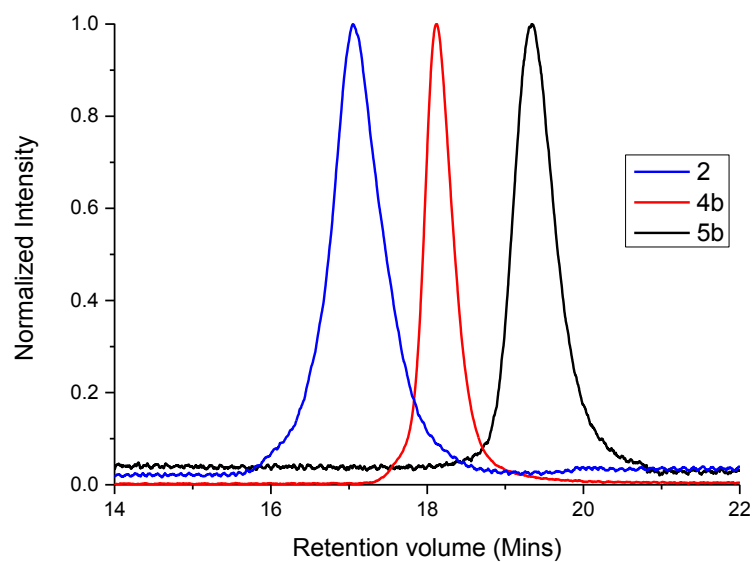
Figure S2. GPC chromatographs (refractive index response) in THF of purified triblock terpolymer **2** (PS$_{388}$-*b*-PFS$_{55}$-*b*-PMMA$_{381}$), and its precursors **4b** (PS$_{388}$-*b*-PFS$_{55}$) and **5b** (PMMA$_{381}$).
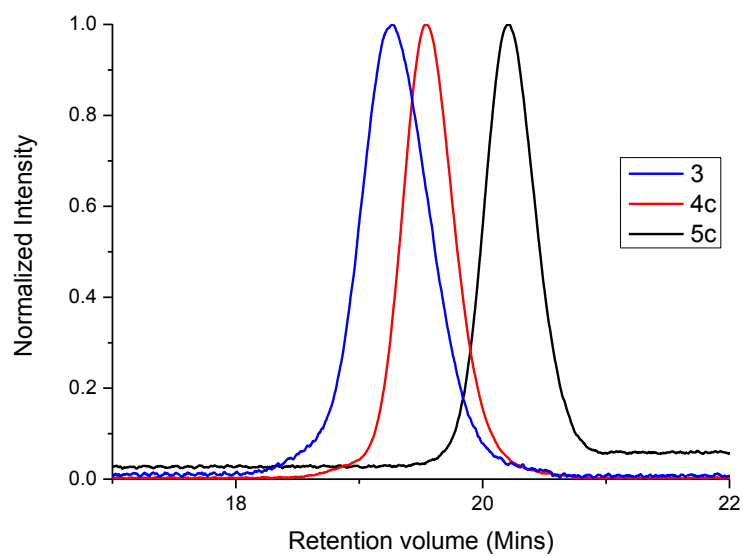
Figure S3. GPC chromatographs (refractive index response) in THF of purified triblock terpolymer **3** (PS$_{53}$-*b*-PFS$_{49}$-*b*-PMMA$_{70}$), and its precursors **4c** (PS$_{53}$-*b*-PFS$_{49}$) and **5c** (PMMA$_{70}$).
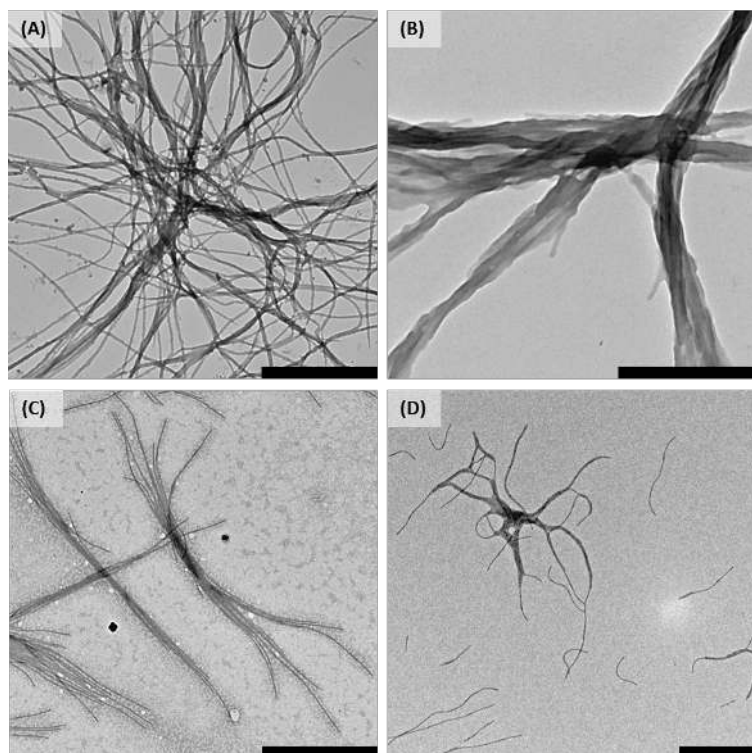
Figure S4. TEM micrographs of micelles of composed of **1** (PS$_{143}$-*b*-PFS$_{40}$-*b*-PMMA$_{188}$) drop-cast after

48 h from (A), (B) DMAA (B is a high magnification image showing the tape-like structures afforded),

(C) EtOAc and (D) acetone. Scale bars are (A), (C) and (D) 2000 nm; (B) 500 nm.
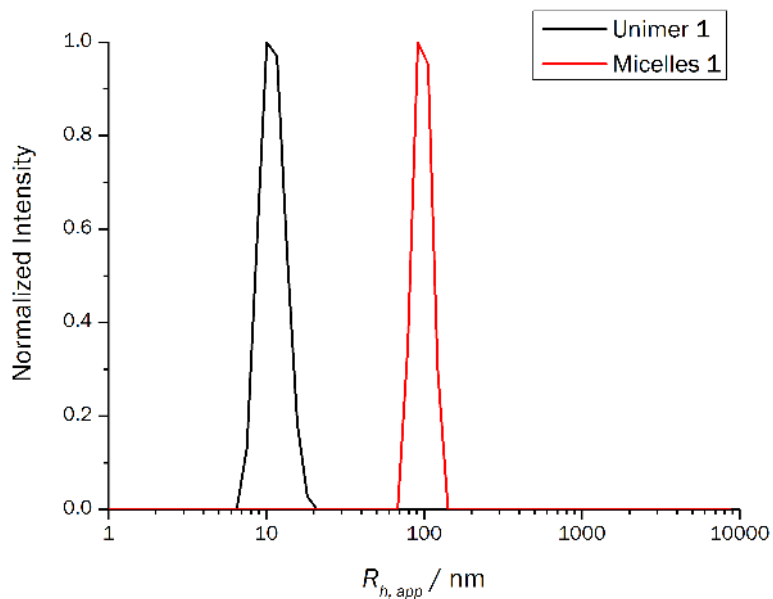
Figure S5. DLS data for unimeric and micellar solutions of **1** (PS$_{143}$-*b*-PFS$_{40}$-*b*-PMMA$_{188}$, in THF (black trace) and acetone (red trace) respectively).

The self-assembly behavior of **1** in acetone was monitored by dynamic light scattering (DLS), which confirmed the formation of assemblies with an apparent hydrodynamic radius ($R_{h,app}$) of 91 nm in acetone, compared to that observed for the unimer ($R_{h,app}$ = 11 nm) in THF.
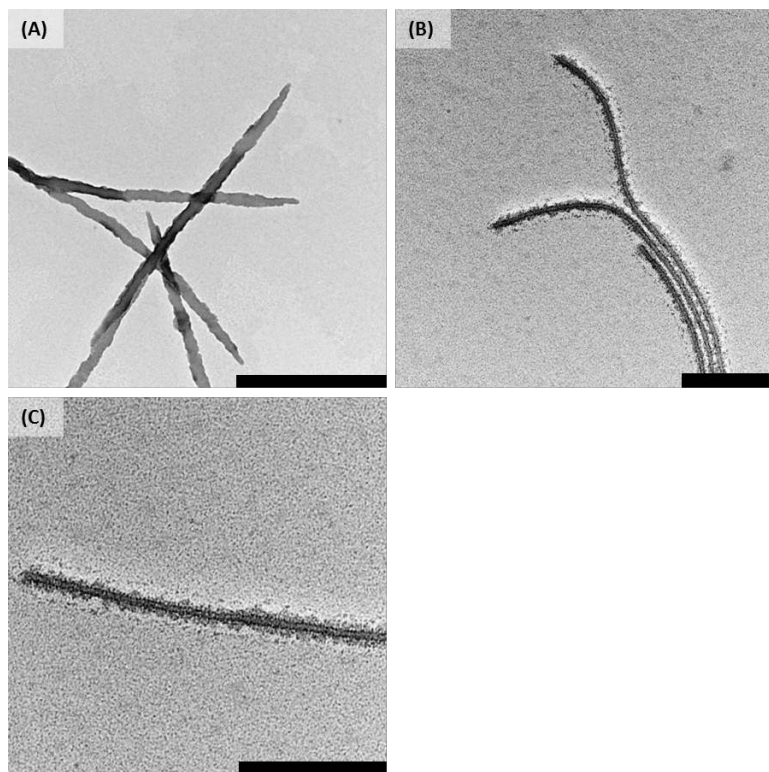
Figure S6. (A) TEM micrograph of micelles of **1** (PS_{143}-*b*-PFS_{40}-*b*-$PMMA_{188}$) drop-cast from DMAA and subsequently stained with RuO_4, showing no evidence for segregation of the PS and PMMA coronal chains; (B), (C) additional TEM micrograph images of cylindrical micelles of **1** drop-cast from acetone and subsequently exposed to RuO_4, revealing a compartmentalized coronal structure. Scale bars are (A) 1000 nm; (B)-(C) 200 nm.
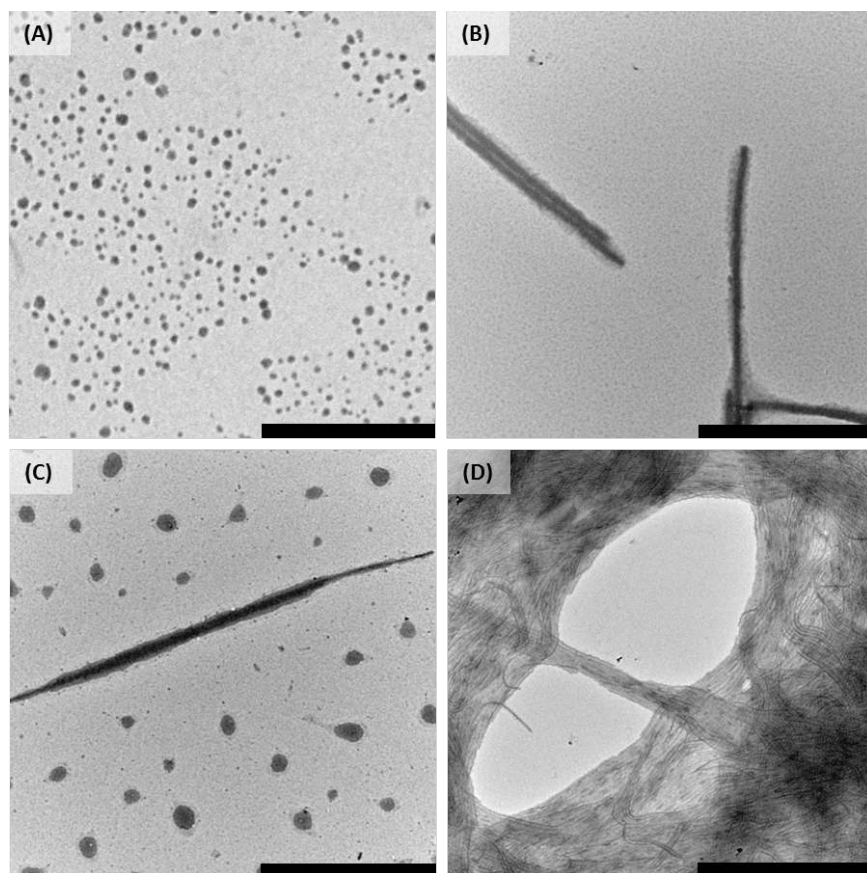
Figure S7. TEM micrographs of micelles composed of **2** (PS$_{381}$-*b*-PFS$_{55}$-*b*-PMMA$_{388}$) drop-cast from (A) DMAA after 48 h, (B) DMAA after 14 d, (C) EtOAc after 48 h and (D) acetone after 48 h. Scale bars are (A) 1000 nm; (B)-(D) 2000 nm.
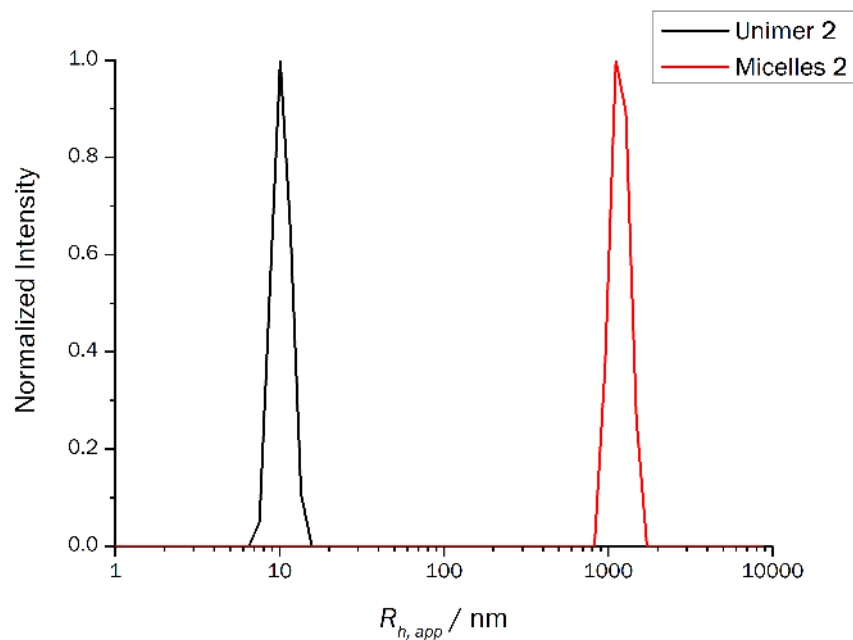
Figure S8. DLS data for unimeric and micellar solutions of **2** (PS$_{381}$-*b*-PFS$_{55}$-*b*-PMMA$_{388}$, in THF (black trace) and acetone (red trace) respectively).

The formation of micelles was confirmed by DLS, with the aforementioned structures of **2** having a $R_{h,app}$ of 1280 nm in acetone.
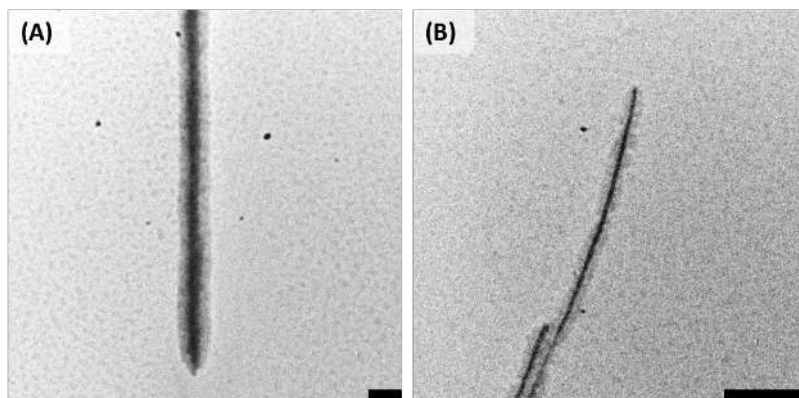
Figure S9. TEM micrograph of micelles of **2** (PS$_{381}$-*b*-PFS$_{55}$-*b*-PMMA$_{388}$) drop-cast from (A) DMAA and (B) EtOAc and subsequently stained with RuO$_4$, showing no discernible, and poorly-defined coronal compartmentalization in DMAA and EtOAc, respectively. Scale bars are 200 nm.
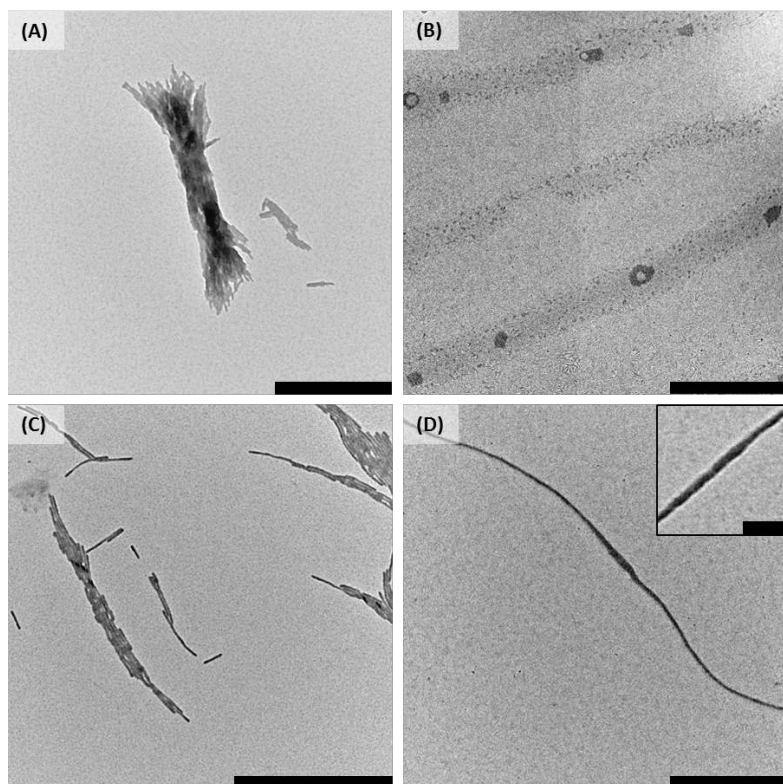
Figure S10. TEM micrographs of micelles composed of **3** (PS$_{53}$-*b*-PFS$_{49}$-*b*-PMMA$_{70}$) drop-cast after 48 h from (A) DMAA, (B) EtOAc, (C) acetone and (D) (and inset) acetone/EtOAc (1:1 (v/v)). Scale bars are (A)-(D) 1000 nm, (D inset) 200 nm.
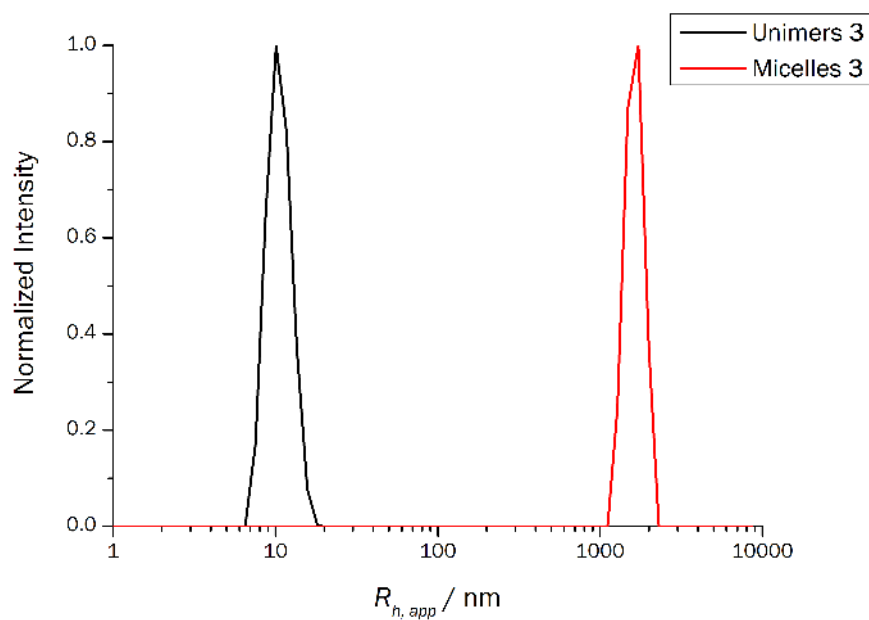
Figure S11. DLS data for unimeric and micellar solutions of **3** (PS$_{53}$-*b*-PFS$_{49}$-*b*-PMMA$_{70}$, in THF and acetone respectively).

The formation of micelles was confirmed by DLS, with the aforementioned structures having a $R_{h,app}$ of 1032 nm in acetone.
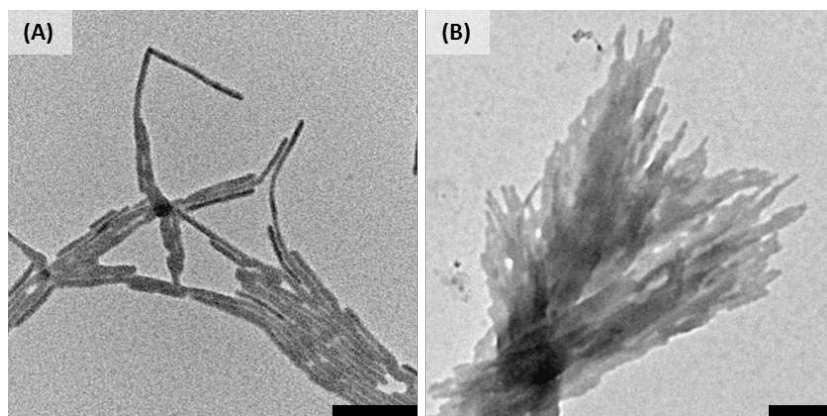

Figure S12. Showing non-patchy nature of corona of **3** (PS$_{53}$-*b*-PFS$_{49}$-*b*-PMMA$_{70}$) in acetone and DMAA. Scale bars are 200 nm.
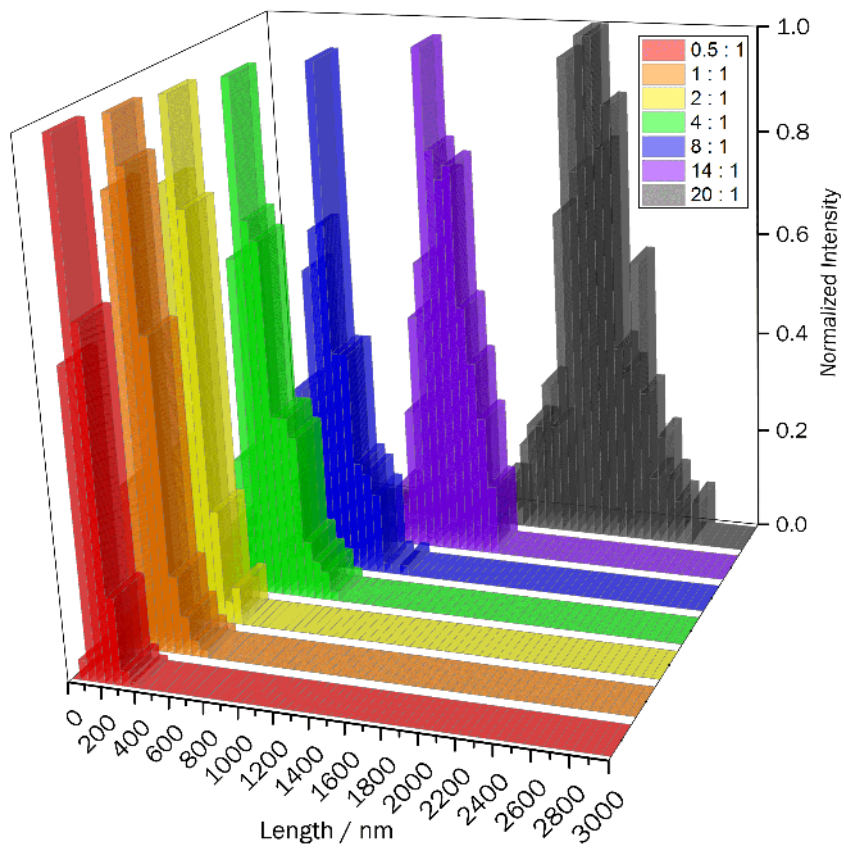
Figure S13. Histograms showing the contour length distribution of cylindrical micelles of **1** (PS$_{143}$-*b*-PFS$_{40}$-*b*-PMMA$_{188}$) prepared by living CDSA seeded growth methods. Legend in the top right denotes the unimer-to-seed ratio.
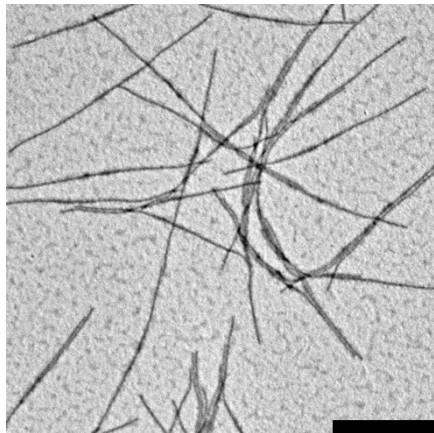
Figure S14. TEM micrograph of monodisperse cylindrical micelles of **1** (PS$_{143}$-*b*-PFS$_{40}$-*b*-PMMA$_{188}$) drop-cast from acetone prepared by "living" CDSA by the addition of 20 equivalents of unimer and left to age for 7 d, showing the lingering presence of film presumably derived from unassembled unimer of **1**. Scale bar is 1000 nm.
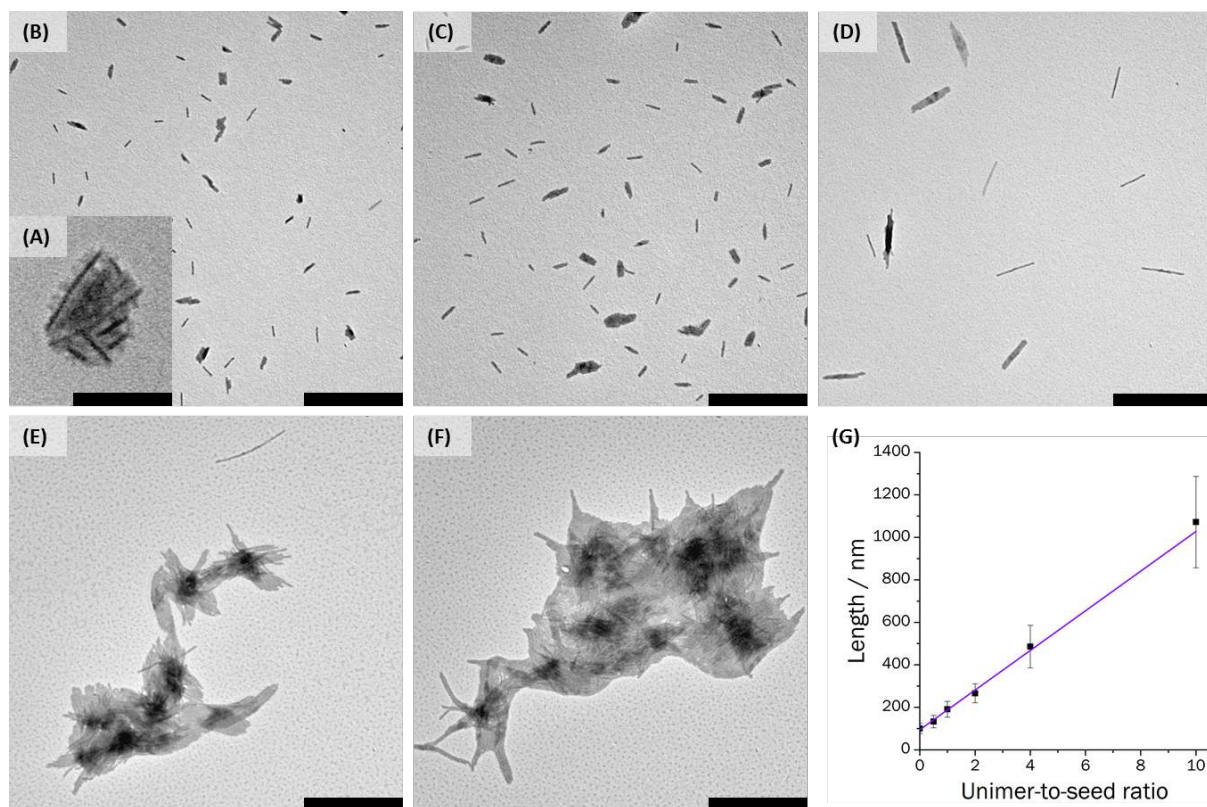
Figure S15. (A) TEM micrographs of seed micelles of **2** (PS_{381}-*b*-PFS_{55}-*b*-$PMMA_{388}$) prepared by sonication for 2 h at 0 °C in acetone (L_n = 101 nm, L_w/L_n = 1.14); (B)-(F) TEM micrographs of monodisperse cylindrical micelles drop-cast from acetone prepared by "living" CDSA by the addition of (B) 1, (C) 2, (D) 4, (E) 10 and (F) 20 equivalents of unimer **2**.; G graph showing the linear dependence of micelle length to the unimer-to-seed ratio of **2**. Scale bars are (A) 200 nm; (B)-(F) 2000 nm.
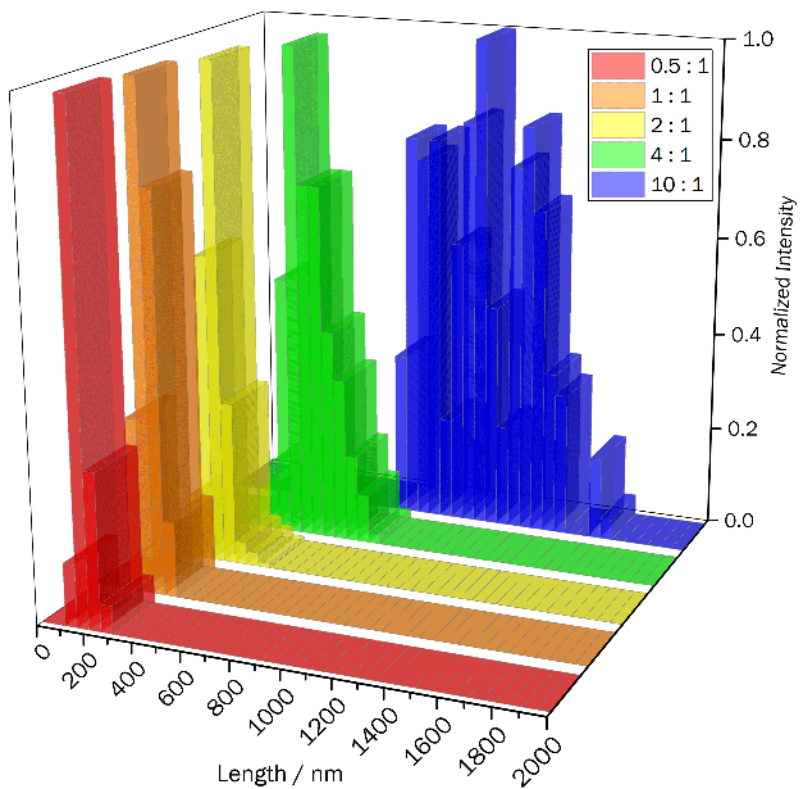
Figure S16. Histograms showing the contour length distribution of cylindrical micelles of **2** (PS$_{381}$-*b*-PFS$_{55}$-*b*-PMMA$_{388}$) prepared by living CDSA seeded growth methods. Legend in the top right denotes the unimer-to-seed ratio.

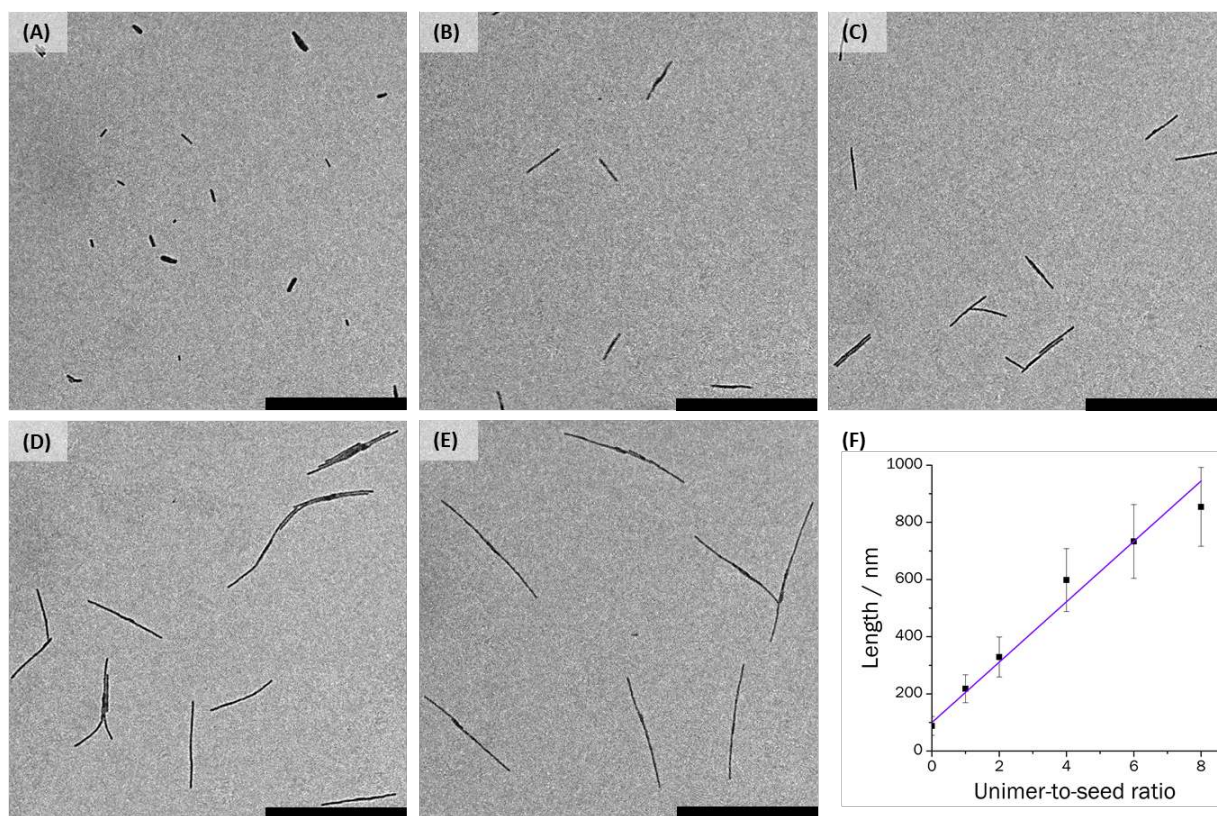**Figure S17**. (A) TEM micrograph of seed micelles of **3** (PS_{53}-*b*-PFS_{49}-*b*-$PMMA_{70}$) prepared by sonication for 2 h at 0 °C in acetone (L_n = 88 nm, L_w/L_n = 1.09); (B)-(F) TEM micrographs of monodisperse cylindrical micelles of **3** drop-cast from acetone prepared by "living" CDSA by the addition of (B) 1, (C) 2, (D) 4 and (E) 8 equivalents of unimer **3**.; (F) graph showing the linear dependence of micelle length to the unimer-to-seed ratio of **3**. Scale bars are 1000 nm.
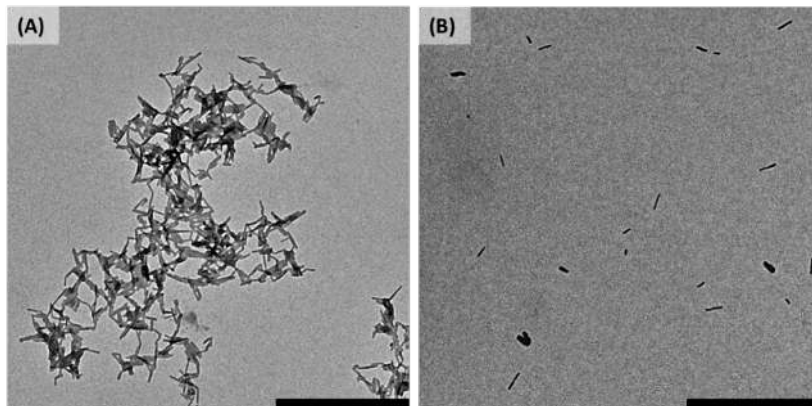
Figure S18. TEM micrographs of seed micelles of **3** (PS_{53}-*b*-PFS_{49}-*b*-$PMMA_{70}$) when drop-cast (A) from acetone and (B) when diluted with butyl acetate (1:1 (v/v)). Scale bars are 1000 nm.
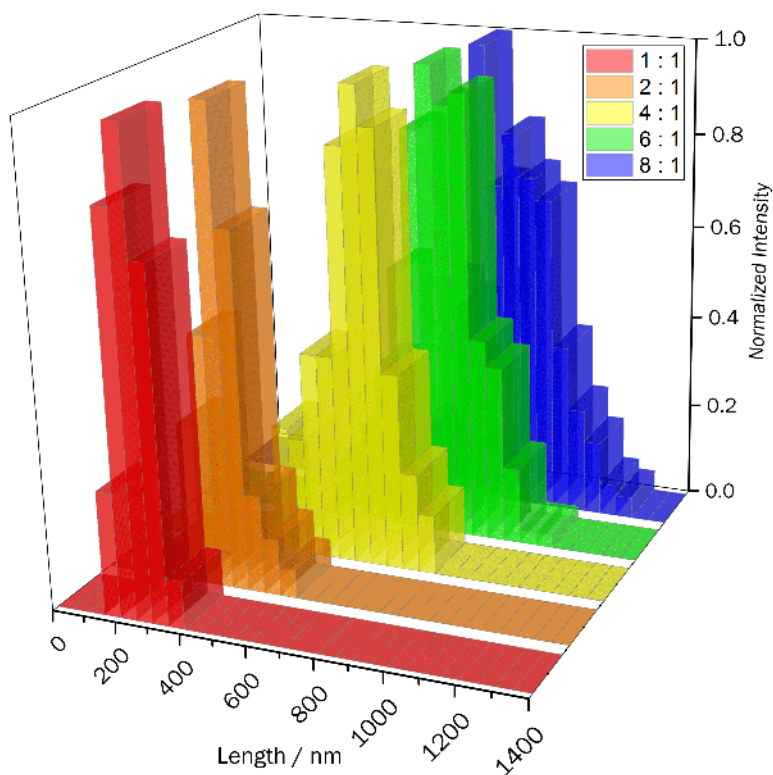
Figure S19. Histograms showing the contour length distribution of cylindrical micelles of **3** (PS$_{53}$-*b*-PFS$_{49}$-*b*-PMMA$_{70}$) prepared by living CDSA seeded growth methods. Legend in the top right denotes the unimer-to-seed ratio.
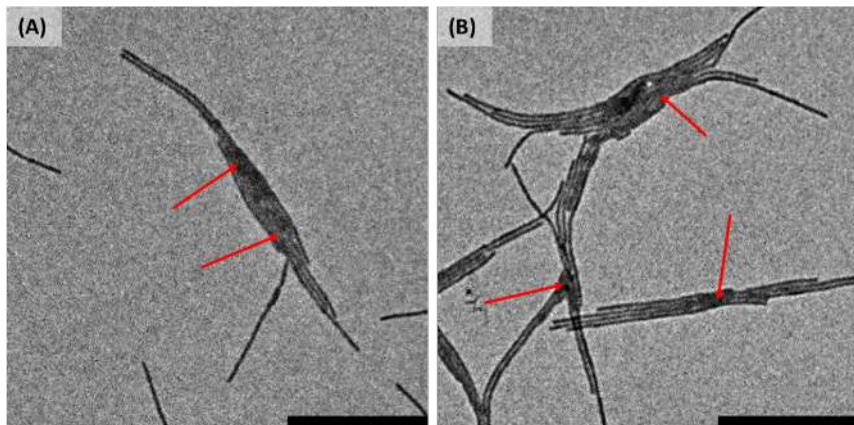
Figure S20. TEM micrographs of **3** (PS$_{53}$-*b*-PFS$_{49}$-*b*-PMMA$_{70}$) drop-cast from acetone showing branching of micelles at unimer-to-seed ratio of (A) 4 and (B) 8. Red arrows indicate branched micelles. Scale bars are 500 nm.
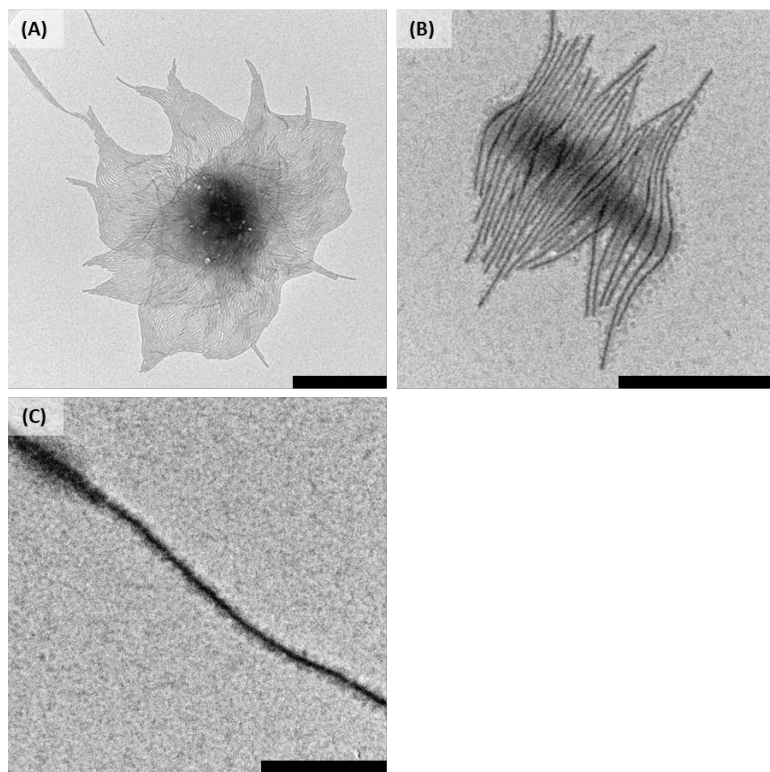
Figure S21. TEM micrographs of block comicelles prepared from monodisperse PFS_{50}-b-$P2VP_{675}$ seed micelles following the addition of unimer **1** (PS_{143}-b-PFS_{40}-b-$PMMA_{188}$) in (A) acetone, (B) EtOAc and (C) acetone/EtOAc (1 : 1 (v/v)). The latter is a magnified TEM micrograph to highlight the "patchy" nature of the coronal chains along the outer blocks of the block comicelle. Scale bars are (A) 2000 nm; (B) 500 nm; (C) 200 nm.
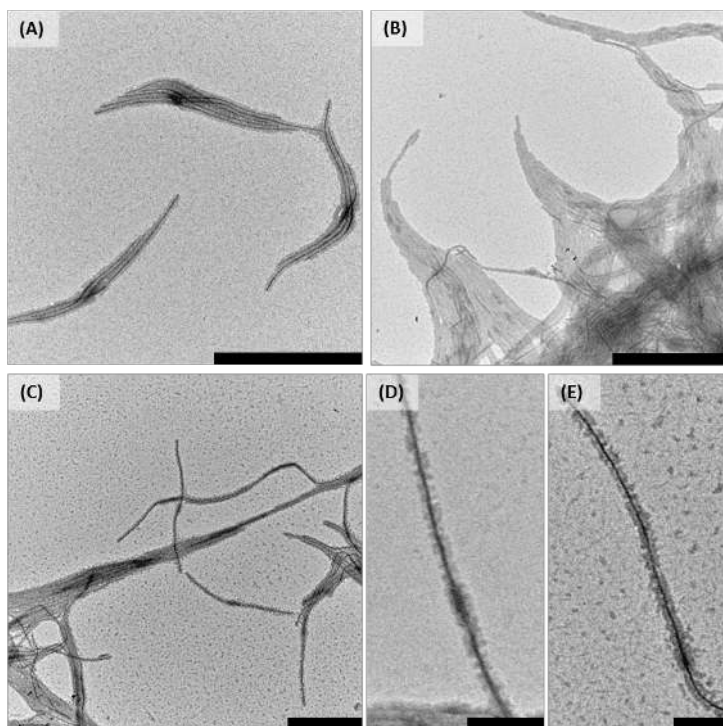
Figure S22. TEM micrographs of block comicelles prepared from monodisperse PFS_{50}-*b*-$P2VP_{675}$ seed micelles following the addition of unimer **2** (PS_{381}-*b*-PFS_{55}-*b*-$PMMA_{388}$) drop-cast from (A) EtOAc, (B) acetone and (C) acetone/EtOAc (1:1 (v/v)); (D) and (E) high resolution TEM micrographs of S12(B) and S12(C) respectively showing the compartmentalization of the coronal chains along the micelle backbone. Scale bars are (A)-(C) 1000 nm; (D) and (E) 200 nm.
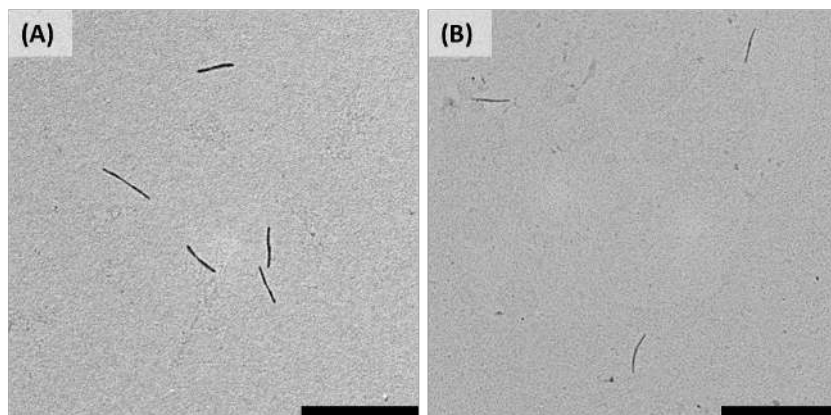
Figure S23. Low magnification TEM micrographs of representative triblock comicelles prepared from monodisperse "patchy" seed micelles when drop-cast from acetone; (A) a triblock comicelle with a central seed segment composed of **1** (PS_{143}-*b*-PFS_{40}-*b*-$PMMA_{188}$), with outer blocks derived from unimers of **2** (PS_{381}-*b*-PFS_{55}-*b*-$PMMA_{388}$); (B) a triblock comicelle with a central seed segment composed of **2**, with outer blocks derived from unimers of **1**. Scale bars are 2000 nm.

REFERENCES

1.   Rider, D. A.; Cavicchi, K. A.; Power-Billard, K. N.; Russell, T. P.; Manners, I., Diblock Copolymers with Amorphous Atactic Polyferrocenylsilane Blocks: Synthesis, Characterization, and Self-Assembly of Polystyrene-block-poly(ferrocenylethylmethylsilane) in the Bulk State. *Macromolecules* **2005,** *38* (16), 6931-6938.

2.   Hansen, C. H., *Hansen Solubility Parameters: A User's handbook*. 1st ed.; CRC Press LLC: Florida, 2000.

3.   Brandup, J., *Polymer Handbook*. 4th ed.; John Wiley & Sons: New York, 2005.

4.   Kulbaba, K.; MacLachlan, M. J.; Evans, C. E. B.; Manners, I., Organometallic Gels: Characterization and Electrochemical Studies of Swellable, Thermally Crosslinked Poly(ferrocenylsilane)s. *Macromol. Chem. Phys.* **2001,** *202* (9), 1768-1775.

5.   Zhang, M.; Rupar, P. A.; Feng, C.; Lin, K.; Lunn, D. J.; Oliver, A.; Nunns, A.; Whittell, G. R.; Manners, I.; Winnik, M. A., Modular Synthesis of Polyferrocenylsilane Block Copolymers by Cu-Catalyzed Alkyne/Azide "Click" Reactions. *Macromolecules* **2013,** *46* (4), 1296-1304.